An Improved Control Strategy using RSC of the Wind Turbine Based on DFIG for Grid Harmonic Currents Mitigation

Moussa Reddak*‡, Abdelmajid Berdai*, Anass Gourma*, Jamal Boukherouaa*

*High national school of electricity and mechanics (ENSEM), Electrical Engineering Department, Hassan II University, 8118 Oasis Casablanca-Morocco

(moussa.reddak@gmail.com, a.berdai@gmail.com, a.gourma@gmail.com, j.boukherouaa@yahoo.fr)

‡ Corresponding author: Moussa Reddak; Route d'El Jadida, km 7, Postal adress: 8118, Oasis, Tel: +2126 222 047, Fax: 522 230789, moussa.reddak@gmail.com

Received: 21.06.2017 Accepted:20.08.2017

Abstract- Due to nonlinear loads integration in the grid, wind turbines type doubly fed induction generator DFIG must contribute with their ancillary services to the improvement of energy quality, especially in the mitigation of harmonic currents imposed by these nonlinear loads. In this paper, the strategy control of the DFIG is not only limited in the optimal powers control, but also ameliorating of harmonic currents mitigation existing in the grid. To achieve this objective, a new nonlinear control strategy based on the integral Backstepping strategy has been proposed to be flexible rotor currents dynamics, and thanks to the contribution of rotor side converter RSC control. This choice presents more advantages compared with the control of the grid side converter GSC as an active filter. The used method in this paper and which serves to identify the harmonic currents is based on synchronous reference frame SRF. The simulation results show the effectiveness of the proposed control strategy which is manifested by a net reduction in the total harmonic distortion THD.

Keywords Wind turbines, harmonic currents mitigation, RSC of DFIG, Control strategy.

1. Introduction

With the emergence of electronic power in the industry such as variable speed drives and the domestic loads equipped with converters or switching power supply, such as microwave ovens, computers, printers, photocopiers, fluorescent lamps, harmonic currents appear in the grid, which cause several problems such as voltage or current distortion and also causing the heating of cables and power systems etc. [1],[2].

In the studied case of the wind energy conversion system, the used generator is a doubly fed induction generator DFIG controlled by a back-to-back converter connected to the rotor circuit; this converter is dimensioned to transit a portion of power output and which is estimated at 30% of the power of the generator. The DFIG allows exploiting wide speed variation interval and an independent control of active and reactive powers [3],[4],[5].

Regarding the ancillary services [6]–[8], the wind energy conversion system equipped with DFIG can be used to compensate the reactive power and the grid harmonic currents. To identify these harmonic currents, two main methods are cited, the first is known as PQ identification method based on calculation of imaginary powers [9]. This method requires two current sensors and two voltage sensors. The second method, called synchronous reference frame (SRF) that only requires two current sensors and uses a low-pass filter [10].

Active filtering is among of appropriate solutions for the grid harmonic currents mitigation [11], [12]. The active filter simultaneously allows to detect and to mitigate the harmonic currents that are imposed by nonlinear loads. In [13] the grid side converter is used as an active filter, the used identification method for harmonic currents is the SRF method. In [14] the reference currents include the identified harmonic current coming from the identification block that use PQ method. In [15], the author has proposed to modify the control system of the RSC by including the function of

active filtering and compensation of the reactive power, the used control strategy is the hysteresis control and the identification is made by the SRF method.

To point out, in the literature of the authors who have studied active filtering have systematically implemented linear controllers type PI in order to regulate the harmonic currents; these controllers are originally used in the conventional control systems. However, this type of controllers cannot accurately regulate the harmonic currents due to their limit bandwidth, because of these controllers are dimensioned to regulate continuous currents in the conventional controls [16],[17].

In this context, the aim of our paper is the ensuring of active filtering by using a DFIG like a filter in addition to powers control. Thus, a new nonlinear control strategy based on integral backstepping control has been proposed, its description is detailed in the FIG 1.After modeling the system (section 2), and the role of the RSC is not limited to the optimal powers control [18] [19], but also to improved compensation of the harmonic currents generated by the nonlinear load connected at PCC. To achieve the function of the active filtering with RSC, the identified harmonic currents are added to rotor reference currents with a negative sign in order to compensate the harmonic currents existing in the grid (section 3). The used identification method in this paper is SRF method that uses just two current sensors (section 4).The simulation results will be described to justify the importance and the effectiveness of the proposed control that allow a net decrease of the THD (section 5).

2. Wind-turbine-DFIG Modelling

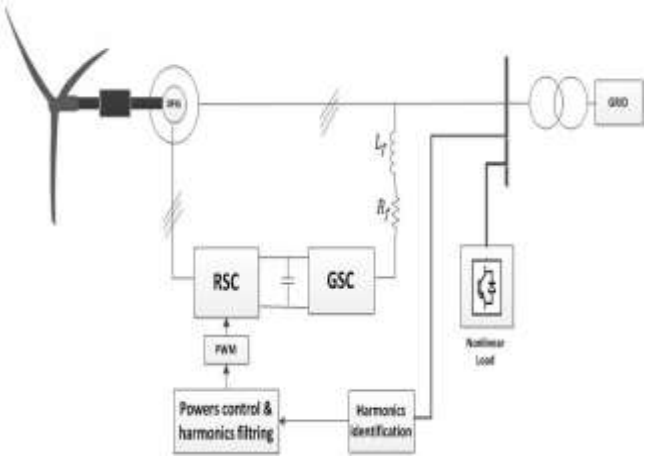

Fig. 1. Description of the system and its strategy control.

In the above system, a DFIG is driven by a wind turbine in order to insure the active filtering function. So, a block identification detect the harmonics currents that is generated by the nonlinear load in order to give it to the block of power control and harmonics filtering, the later block generate the currents references to RSC that drive the DFIG.

2.1. System modelling of wind turbine

According to Betz theory, the captured mechanical power is defined [20]:

$$P_a = \frac{1}{2}\rho\pi R^2 V_w^3 C_p(\lambda,\beta) \tag{1}$$

Its aerodynamic torque is:

$$\mathrm{T_a} = \frac{1}{2}\rho\pi \mathrm{R}^3 \frac{\mathrm{C_p}}{\lambda}\mathrm{V_w^2} \tag{2}$$

While $\mathrm{V_w}$ is the wind speed, $\mathrm{C_p}$ is the power coefficient, R is the rotor radius, β is the pitch angle, λ is the tip-speed ratio, and ρ is the air density.

The dynamic law of the wind turbine is given:

$$\mathrm{J}_{eq}\frac{\mathrm{d}\omega}{\mathrm{dt}} = \mathrm{T_a} - \mathrm{f}_{eq}\omega - \mathrm{T_e} \tag{3}$$

2.2. DFIG modelling

The voltages and the currents expression in the Park reference related to the d-q synchronous field [21] [22], [23] is:

$$\begin{cases} \mathrm{v_{ds}} = \mathrm{R_s i_{ds}} + \frac{\mathrm{d}\varphi_{\mathrm{ds}}}{\mathrm{dt}} - \omega_\mathrm{s}\varphi_{\mathrm{qs}} \\ \mathrm{v_{qs}} = \mathrm{R_s i_{qs}} + \frac{\mathrm{d}\varphi_{\mathrm{qs}}}{\mathrm{dt}} + \omega_\mathrm{s}\varphi_{\mathrm{ds}} \\ \mathrm{v_{dr}} = \mathrm{R_r i_{dr}} + \frac{\mathrm{d}\varphi_{\mathrm{dr}}}{\mathrm{dt}} - \omega_\mathrm{r}\varphi_{\mathrm{qr}} \\ \mathrm{v_{qr}} = \mathrm{R_r i_{qr}} + \frac{\mathrm{d}\varphi_{\mathrm{qr}}}{\mathrm{dt}} + \omega_\mathrm{r}\varphi_{\mathrm{dr}} \end{cases} \tag{4}$$

$$\begin{cases} \varphi_{\mathrm{ds}} = \mathrm{L_s i_{ds}} + \mathrm{M i_{dr}} \\ \varphi_{\mathrm{qs}} = \mathrm{L_s i_{qs}} + \mathrm{M i_{qr}} \\ \varphi_{\mathrm{dr}} = \mathrm{L_r i_{dr}} + \mathrm{M I_{ds}} \\ \varphi_{\mathrm{qr}} = \mathrm{L_r i_{qr}} + \mathrm{M i_{qs}} \end{cases} \tag{5}$$

With$\mathrm{R_s}$, $\mathrm{R_r L_s}$and $\mathrm{L_r}$ are respectively the resistors and the inductors of the stator and the rotor windings, M is the mutual inductance.

The DFIG powers are given as:

$$\begin{cases} \mathrm{P_s} = \mathrm{v_{ds} i_{ds}} + \mathrm{v_{qs} i_{qs}} \\ \mathrm{Q_s} = \mathrm{v_{qs} i_{ds}} - \mathrm{v_{ds} i_{qs}} \end{cases} \tag{6}$$

The electromagnetic torque is defined as:

$$\mathrm{T_{em}} = \mathrm{p}(\varphi_{\mathrm{ds}}\mathrm{i_{qs}} - \mathrm{i_{ds}}\varphi_{\mathrm{qs}}) \tag{7}$$

In case the Park reference which is synchronized to the stator rotating field, the simplified fluxes expression is:

$$\begin{cases} \varphi_{\mathrm{ds}} = \mathrm{L_s i_{ds}} + \mathrm{M i_{dr}} = \varphi_\mathrm{s} \\ \varphi_{\mathrm{qs}} = \mathrm{L_s i_{qs}} + \mathrm{M i_{qr}} = 0 \end{cases} \tag{8}$$

Thus

$$T_{em} = p\varphi_s i_{qs} \quad (9)$$

Neglecting the stator resistance, the dq-axis voltages equations are:

$$\begin{cases} v_{ds} = 0 \\ v_{qs} = \omega_s \varphi_s = v_s \end{cases} \quad (10)$$

Hence the dq-axis stator currents are defined as:

$$\begin{cases} i_{sd} = \frac{\varphi_s}{L_s} - \frac{M}{L_s} i_{dr} \\ i_{sq} = -\frac{M}{L_s} i_{qr} \end{cases} \quad (11)$$

Active and reactive powers are:

$$\begin{cases} P_s = -v_s \frac{M}{L_s} i_{qr} \\ Q_s = v_s \frac{\varphi_s}{L_s} - v_s \frac{M}{L_s} i_{dr} \end{cases} \quad (12)$$

And the electromagnetic torque expression is:

$$T_{em} = -p\varphi_s \frac{M}{L_s} i_{qr} \quad (13)$$

So the dynamic rotor currents can be written as:

$$\begin{cases} \frac{di_{dr}}{dt} = \frac{1}{\sigma L_r}(v_{rd} - R_r i_{rd} + \sigma L_r \omega_r i_{rq}) \\ \frac{di_{rq}}{dt} = \frac{1}{\sigma L_r}(v_{rq} - R_r i_{rq} - \sigma L_r \omega_r i_{rd} - \omega_r \frac{M}{L_s}\varphi_s) \end{cases} \quad (14)$$

2.3. Text Layout for Accepted Papers

The converters dynamics are taken equal to 1

3. Contribution of RSC Control in the Improvement of the Active Filtering Function

3.1. Control strategy of RSC representation

In this new control strategy, the role of the RSC is the DFIG optimal powers control and also the improvement of energy quality by compensating the reactive power and harmonic currents existing in the grid.

With nonlinear load insertion at point of common coupling PCC, harmonic currents appear in the grid, which increase the total harmonics distortion of the currents. Reducing this rate, the harmonic currents should be mitigated.

Figure 2 shows the control strategy of RSC that reflects the implementation of active filtering function. The defined harmonic currents identification by Eqs.(17) and 18 are added to the reference currents in order to achieve the goal of active filtering.

The harmonic currents of the load non-linear are converted to rotor currents according the Eq. (19).

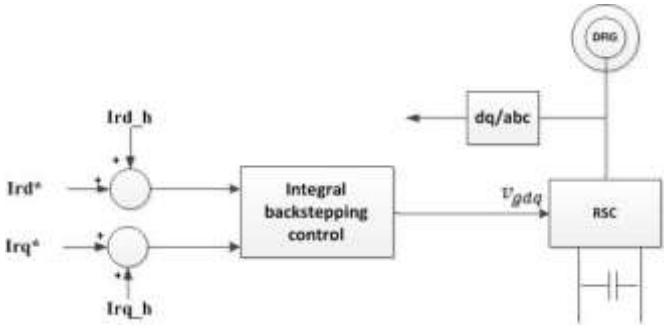

Fig. 2. Strategy control of the RSC.

3.2. Rotor currents references establishing

To include the active filtering in RSC controller, the identified harmonic currents defined by equations (15) and (16) should be added with opposite sign to reference currents defined by equations 17 and 18.

$$I_{rd\_h} = \frac{L_s}{M} I_{cdh\_nL} \quad (15)$$

$$I_{rq\_h} = \frac{L_s}{M} I_{cqh\_nL} \quad (16)$$

$$i_{dr}{}^* = \frac{\varphi_s}{M} - Q_s{}^* \frac{L_s}{M v_s} \quad (17)$$

$$i_{qr}{}^* = -\frac{L_s}{pM\varphi_s} T_{em}{}^* \quad (18)$$

So the resulting references currents are given by:

$$\begin{cases} i_{rd\_ref} = i_{dr}{}^* + I_{rd\_h} \\ i_{rq_{ref}} = i_{qr}{}^* + I_{rq\_h} \end{cases} \quad (19)$$

3.3. Integral backstepping control strategy of RSC

- i_{rd} Current loop:

The i_{rd} tracking error is defined as:

$$Z_d = i_{rd\_ref} - i_{rd} + K_d \int_0^t i_{rd\_ref} - i_{rd}\, dt \quad (20)$$

Lyapunov candidate function is given as:

$$V_d = \frac{1}{2} Z_d{}^2 \quad (21)$$

$$\dot{V}_d = Z_d \dot{Z}_d \quad (22)$$

Substituting the suitable terms, the Lyaponov function derivative is:

$$\dot{V}_d = Z_d \left(\left(i_{rd\_ref} - \frac{1}{\sigma L_r} v_{rd} + \frac{1}{\sigma L_r} R_r i_{rd} + \frac{1}{\sigma L_r} e_q \right) + K_d (i_{rd\_ref} - i_{rd}) + K'_d Z_d \right) - K'_d Z_d{}^2 \quad (23)$$

By taking into account the voltage control input v_{rd} is:

$$v_{rd} = \sigma L_r(\mathrm{i}_{rd\_ref} + K_d(\mathrm{i}_{rd\_ref} - \mathrm{i}_{rd}) + K'_d Z_d) + R_r \mathrm{i}_{rd} + e_q \quad (24)$$

So

$$\dot{V}_d = -K'_d {Z_d}^2 \quad (25)$$

- i_{rq} Current loop

The i_{rq} tracking error is:

$$Z_q = \mathrm{i}_{rq\_ref} - \mathrm{i}_{rq} + K_q \int_0^t \mathrm{i}_{rq\_ref} - \mathrm{i}_{rq}\, dt \quad (26)$$

Lyapunov function will be defined as:

$$V_q = \frac{1}{2} {Z_q}^2 \quad (27)$$

Its derivative

$$\dot{V}_q = Z_q \dot{Z}_q \quad (28)$$

$$\dot{V}_q = Z_q \left(\left(\mathrm{i}_{rq\_ref} - \frac{1}{\sigma L_r} v_{rq} + \frac{1}{\sigma L_r} R_r \mathrm{i}_{rq} + \frac{1}{\sigma L_r} e_d + \frac{1}{\sigma L_r} e_\varphi \right) + K_q(\mathrm{i}_{rq\_ref} - \mathrm{i}_{rq}) + K'_q Z_q \right) - K'_q {Z_q}^2 \quad (29)$$

By taking into account the voltage control input v_{rq} is:

$$v_{rq} = \sigma L_r(\mathrm{i}_{rq\_ref} + K_q(\mathrm{i}_{rq\_ref} - \mathrm{i}_{rq}) + K'_q Z_q) + R_r \mathrm{i}_{rq} + e_d + e_\varphi \quad (30)$$

By substituting this voltage control in Eq. (29), the derivative of Lyaponov function is given as:

$$\dot{V}_q = -K'_q {Z_q}^2 \quad (31)$$

4. Harmonics Isolation

To identify the harmonic currents, the most proposed method in the literature is PQ theory method, it consist to calculate the active and reactive power, then to extract the harmonic currents by using a high-pass filter (HPF) and/or low-pass Filter (LPF). This compound method is complex requires the measures of the current and voltage.

The second method that is proposed in this paper is the SRF Method [16], this method is described in fig. 3. It can be observed that only the currents are measured then the dq harmonic components are extracted by using a low-pass filter.

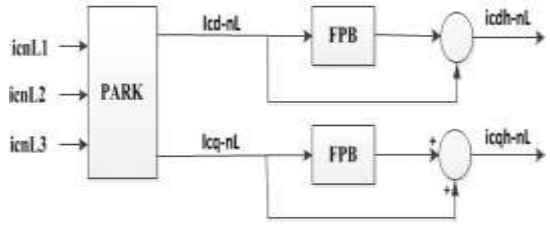

Fig. 3. SRF method for harmonics identification.

5. Simulation Results

To validate the performance of the proposed control strategy allowing active filter function for harmonic currents compensation, simulations are carried out under MATLAB/Simulink. Fig. 1 shows the block diagram of the proposed control system that is composed of a DFIG whose parameters are listed in the table 1, two low pass filters of quality factor of 0.7 have been used in the harmonic currents identification block, and two linear and nonlinear loads representing respectively an inductor and a three-phase rectifier supplying an inductive load.

The control strategy used in this article is a nonlinear control based on integral backstepping; this strategy is used to overcome the problems of the conventional PI control, which is responsible to drawbacks coming from the bound bandwidth unable to deal effectively with the harmonic currents.

Two cases of carried out simulations have been shown: In the first case, the DFIG provides its active and reactive powers without harmonic currents mitigation, so the identified harmonic currents are not added to the reference currents. While in the second case, the simulations show the same measures with harmonic currents compensation.

5.1. Case of simulation without active filtering function

In the first case, the dq-axis rotor currents are shown in Figures 4 and 5.

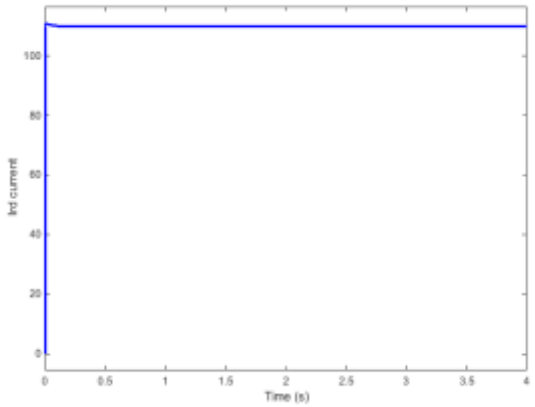

Fig.4. D-axis rotor current without active filtering.

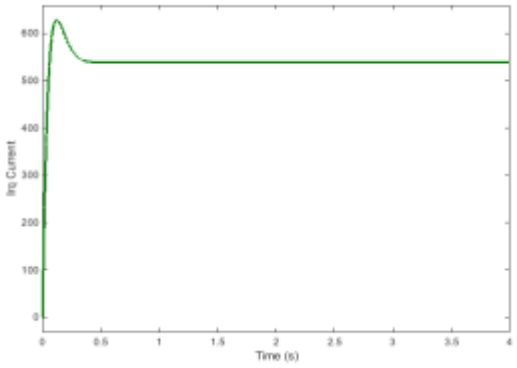

Fig.5. Q-axis rotor current without active filtering.

It can be noted that these currents are smooth because it controls active and reactive powers without active filtering.

In order to evaluate the impact of harmonic currents that cause waveform deformations in the load voltage that represents consumers connected at the PCC, total harmonic distortion (THD) should be calculated and its expression is the following:

$$THD = \frac{100}{I_1}\sqrt{\sum_{h=2}^{\infty} {I_h}^2} \qquad (31)$$

With I_h : the harmonic currents and I_1 : the fundamental.

Figure 6 shows the current absorbed by the nonlinear load and its spectrum. The waveform is distorted and the spectrum shows a THD of 23.72%. On the other hand, fig. 7 shows the THD at PCC with a rate of 15.80%. According to the grid code standard, the THD must be limited by the value of 5%.

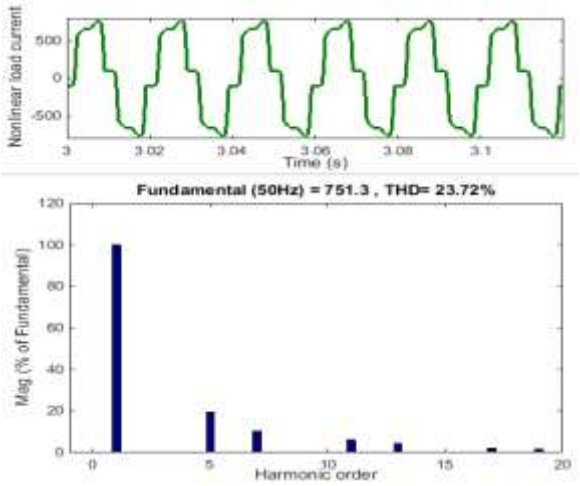

Fig.6. Waveform and spectrum of the load.

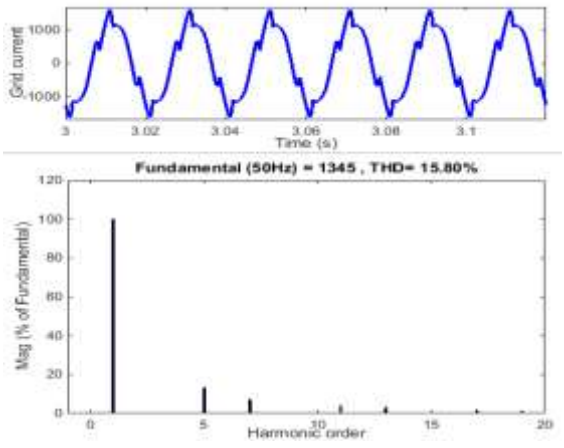

Fig.7. Waveform and spectrum of grid current without active filtering.

The DFIG currents are shown in fig.8.

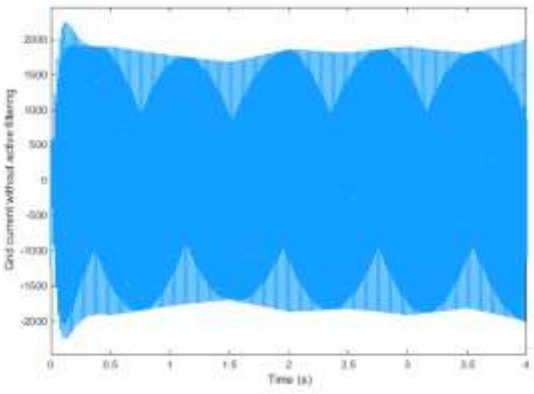

Fig.8. DFIG current without active filtering.

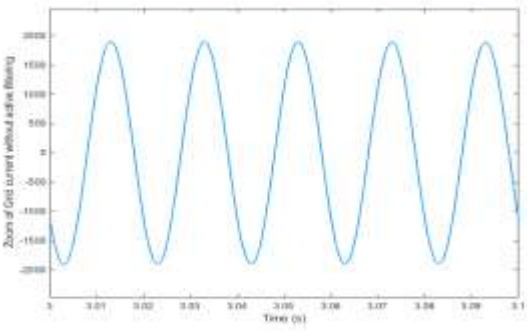

Fig.9. Zoom of DFIG current without active filtering.

Figure 9 shows the zoom of the normal DFIG currents generated to grid without active filtering.

5.2. Case of simulation with active filtering function

In the case of active filtering, after the addition of the harmonic currents coming from the identification block to the reference currents, the dq-axis rotor currents that control active and reactive power are shown in Fig.10 and Fig. 12. The current generated by the DFIG is shown in Fig. 15 and the spectrum of the current circulating in the grid after compensation is shown in Fig. 16. In this case, the obtained grid current THD is 3.93%, which conforms to the standard of the grid code.

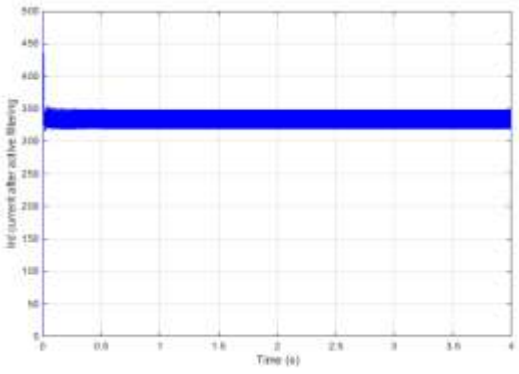

Fig.10. D-axis rotor current with active filtering.

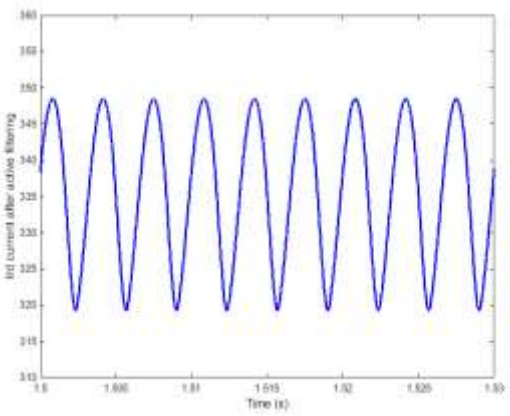

Fig.11. Zoom of d-axis rotor current with active filtering.

Figure 10 show the d-axis rotor current and fig.11 its zoom.

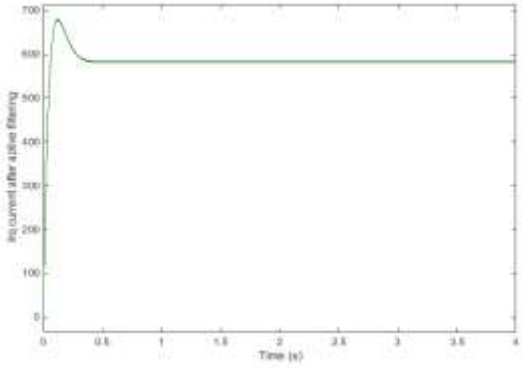

Fig.12. Q-axis rotor current with active filtering.

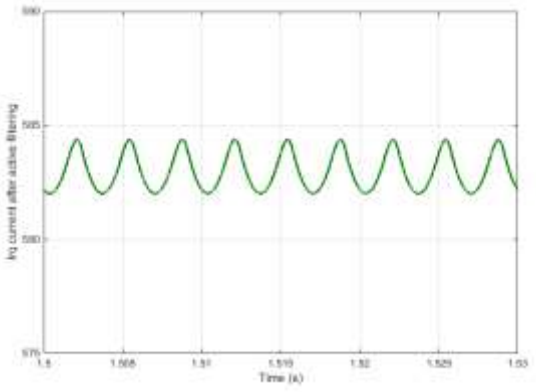

Fig.13. Zoom of q-axis rotor current with active filterin.g

Figure 12 and gives the q-axis current and fig.13 shows its zoom. It can be well-known that these currents contain the harmonics currents references given by the identification block.

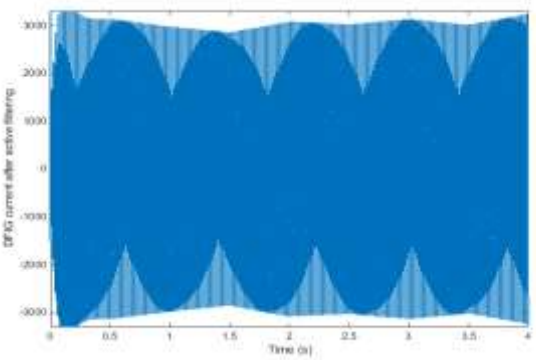

Fig.14. DFIG current with active filtering

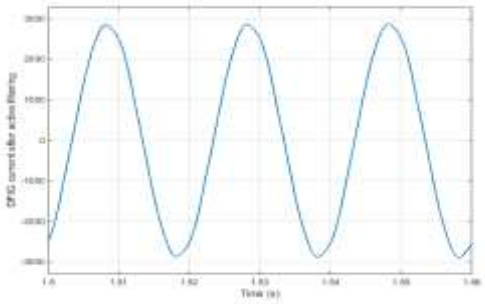

Fig.15. Zoom of DFIG current with active filtering.

Figures 14 and 15 show the DFIG currents that are generated to the grid in the case of active filtering. These later indicate some fluctuation because it compensates the nonlinear load harmonics currents.

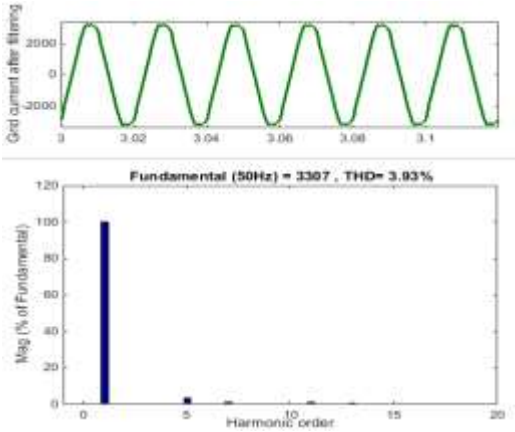

Fig.16. Waveform and spectrum of grid current with active filtering.

In terms of comparison, and based on the simulation results that assess the THD with and without active filtering, the used control strategy for harmonic currents mitigation has been well validated and the obtained THD conforms effectively to the standard of grid code.

To endorse this work, the achieved THD is less than his homologue that is reached in [10].

DFIG characteristics		
Parameters	***Description***	***Values***
P	Power (MW)	2
L_s	Stator inductance (mH)	0.62
L_r	Rotor inductance (mH)	0.62
M	Mutual inductance (mH)	0.3
R_r	Rotor resistance (Ω)	0.025
P	Number of pole pairs	2
v_s	Voltage level (V)	690
f_s	Frequency (Hz)	50

6. Conclusion

In this paper, a new control strategy has been proposed and discussed in order to improve the compensation of harmonic currents generated by nonlinear loads connected to grid. The involvement of RSC control has allowed DFIG rotor currents control in the aim of decreasing the THD grid harmonic currents. This choice is justified by the passage from the stator to the rotor, which means that the identified harmonic currents at PCC are rotor currents' functions, taking into account the DFIG parameters, these identified currents (added to reference currents) have been reduced to optimize the control system.

The proposed control strategy was tested by simulation in Matlab/Simulink. In the first case, the system has been used without active filtering function, whereas in the second case, the new nonlinear control strategy has been contributed to the harmonic currents mitigation. So, the THD has been increased from 15.80% to 3.93%, which confirms the effectiveness of the proposed control strategy that has given a THD conforms to the standard of the grid code. In addition, this control strategy has resolved the problem harmonic currents of the conventional control that requires a limited bandwidth, which have regulated the rotor currents dynamics with precision and robustness.

Acknowledgements

I would like to think the members of our ENSEM laboratory (ESE) for their helps and their clarifications

References

[1] A. Hoseinpour, S. Masoud Barakati, and R. Ghazi, "Harmonic reduction in wind turbine generators using a Shunt Active Filter based on the proposed modulation technique," *Int. J. Electr. Power Energy Syst.*, vol. 43, no. 1, pp. 1401–1412, Dec. 2012.

[2] P. Xiong and D. Sun, "Backstepping-Based DPC Strategy of a Wind Turbine-Driven DFIG Under Normal and Harmonic Grid Voltage," *IEEE Trans. Power Electron.*, vol. 31, no. 6, pp. 4216–4225, Jun. 2016.

[3] M. Cheng and Y. Zhu, "The state of the art of wind energy conversion systems and technologies: A review," *Energy Convers. Manag.*, vol. 88, pp. 332–347, Dec. 2014.

[4] Z. Chen and H. Li, "Overview of different wind generator systems and their comparisons," *IET Renew. Power Gener.*, vol. 2, no. 2, pp. 123–138, Jun. 2008.

[5] D. P. Kadam and B. E. Kushare, "Overview of different wind generator systems and their comparisons," *Int. J. Eng. Sci. Adv. Technol.*, vol. 2, no. 4, pp. 1076–1081, 2012.

[6] S. D. K. Varma, Y. P. Obulesh, and C. Saibabu, "An Improved Synchronous Reference Frame Controller Based Dynamic Voltage Restorer for Grid Connected Wind Energy System," vol. 6, no. 3, 2016.

[7] Y. Krim, S. Krim, and M. F. Mimouni, "Control of a Wind Farm Connected to the Grid at a Frequency and Variable Voltage," *Int. J. Renew. ENERGY Res.*, vol. 6, no. 3, pp. 747–758, 2016.

[8] G. Brando, L. P. Di Noia, R. Rizzo, D. Lauria, and C. Pisani, "An advanced system for power supply and power quality improvement of isolated AC passive network," *2015 Int. Conf. Renew. Energy Res. Appl. ICRERA 2015*, vol. 5, pp. 1446–1450, 2015.

[9] L. Asiminoael, F. Blaabjerg, and S. Hansen, "Detection is key-Harmonic detection methods for active power filter applications," *IEEE Ind. Appl. Mag.*, vol. 13, no. 4, pp. 22–33, 2007.

[10] A. K. Jain and V. T. Ranganathan, "Wound Rotor Induction Generator With Sensorless Control and Integrated Active Filter for Feeding Nonlinear Loads in a Stand-Alone Grid," *IEEE Trans. Ind. Electron.*, vol. 55, no. 1, pp. 218–228, Jan. 2008.

[11] X. D. X. D *et al.*, "&xuuhqw +duprqlfv 0lwljdwlrq xvlqj d 0rgxodu 0xowlohyho &rqyhuwhu %dvhg 6kxqw $fwlyh 3rzhu)lowhu," vol. 5, pp. 6–10, 2016.

[12] M. S. Hamad, K. H. Ahmed, and A. S. Abdel-Khalik, "Grid connected high power medium voltage wind energy conversion system with reduced line harmonics," *2015 Int. Conf. Renew. Energy Res. Appl. ICRERA 2015*, pp. 1279–1284, 2015.

[13] A. B. Moreira, T. A. S. Barros, V. S. C. Teixeira, and E. Ruppert, "Power control for wind power generation and current harmonic filtering with doubly fed induction generator," *Renew. Energy*, vol. 107, pp. 181–193, Jul. 2017.

[14] R. Dehini, A. Bassou, and B. Ferdi, "Artificial neural networks application to improve shunt active power filter," *Int. J. Comput. Inf. Eng.*, vol. 3, no. 4, pp. 247–254, 2009.

[15] M. Kesraoui, A. Chaib, A. Meziane, and A. Boulezaz, "Using a DFIG based wind turbine for grid current harmonics filtering," *Energy Convers. Manag.*, vol. 78, pp. 968–975, Feb. 2014.

[16] A. Gaillard, P. Poure, S. Saadate, and M. Machmoum, "Variable speed DFIG wind energy system for power generation and harmonic current mitigation," *Renew. Energy*, vol. 34, no. 6, pp. 1545–1553, Jun. 2009.

[17] M. Boutoubat, L. Mokrani, and M. Machmoum, "Control of a wind energy conversion system equipped by a DFIG for active power generation and power quality improvement," *Renew. Energy*, vol. 50, pp. 378–386, Feb. 2013.

[18] M. Reddak, A. Berdai, A. Gourma, and A. Belfqih, "Integral backstepping control based maximum power point tracking strategy for wind turbine systems driven DFIG," in *Electrical and Information Technologies (ICEIT), 2016 International Conference on*, 2016, pp. 84–88.

[19] A. M. Rahim Ajabi-Farshbaf, Mohammad Reza Azizian, Sirvan Shazdeh, "Modelling of a New Configuration for DFIGs Using T-type Converters and a Predictive Control Strategy in Wind Energy ... Modeling of a New Configuration for DFIGs Using T-type Converters and a Predictive Control Strategy in Wind Energy Conversion Systems," *Int. J. Renew. ENERGY Res.*, vol. 6, no. 3, pp. 975–956, 2016.

[20] T. Ghennam, K. Aliouane, F. Akel, B. Francois, and E. M. Berkouk, "Advanced control system of DFIG based wind generators for reactive power production and integration in a wind farm dispatching," *Energy Convers. Manag.*, vol. 105, pp. 240–250, Nov. 2015.

[21] V. R. R. Rudraraju, C. Nagamani, and G. S. Ilango, "A control scheme for improving the efficiency of DFIG at low wind speeds with fractional rated converters," *Int. J. Electr. Power Energy Syst.*, vol. 70, pp. 61–69, Sep. 2015.

[22] N. Sarma, J. M. Apsley, and S. Djurović, "Implementation of a conventional DFIG stator flux oriented control scheme using industrial converters," *2016 IEEE Int. Conf. Renew. Energy Res. Appl. ICRERA 2016*, vol. 5, pp. 236–241, 2017.

[23] E. Aydin, A. Polat, and L. T. Ergene, "Vector control of DFIG in wind power applications," *2016 IEEE Int. Conf. Renew. Energy Res. Appl.*, vol. 5, no. 1, pp. 478–483, 2016.